A Novel Conotoxin Inhibitor of Kv1.6 Channel and nAChR Subtypes Defines a New Superfamily of Conotoxins[†,‡]

Julita S. Imperial,[*,§,||] Paramjit S. Bansal,[||] Paul F. Alewood,[||] Norelle L. Daly,[||] David J. Craik,[||] Annett Sporning,[⊥] Heinrich Terlau,[⊥,@] Estuardo López-Vera,[§] Pradip K. Bandyopadhyay,[§] and Baldomero M. Olivera[§]

Department of Biology, University of Utah, Salt Lake City, Utah 84112, Institute for Molecular Bioscience, The University of Queensland, Brisbane, QLD 4072, Australia, Molecular and Cellular Neuropharmacology Group, Max-Planck-Institute for Experimental Medicine, D-37075 Göttingen, Germany, and Institute for Experimental and Clinical Pharmacology and Toxicology, Universitaetsklinikum Schleswig-Holstein, D-23538 Luebeck, Germany

Received February 7, 2006; Revised Manuscript Received April 28, 2006

ABSTRACT: Using assay-directed fractionation of the venom from the vermivorous cone snail *Conus planorbis*, we isolated a new conotoxin, designated pl14a, with potent activity at both nicotinic acetylcholine receptors and a voltage-gated potassium channel subtype. pl14a contains 25 amino acid residues with an amidated C-terminus, an elongated N-terminal tail (six residues), and two disulfide bonds (1−3, 2−4 connectivity) in a novel framework distinct from other conotoxins. The peptide was chemically synthesized, and its three-dimensional structure was demonstrated to be well-defined, with an α-helix and two 3_{10}-helices present. Analysis of a cDNA clone encoding the prepropeptide precursor of pl14a revealed a novel signal sequence, indicating that pl14a belongs to a new gene superfamily, the J-conotoxin superfamily. Five additional peptides in the J-superfamily were identified. Intracranial injection of pl14a in mice elicited excitatory symptoms that included shaking, rapid circling, barrel rolling, and seizures. Using the oocyte heterologous expression system, pl14a was shown to inhibit both a K^+ channel subtype (Kv1.6, IC_{50} = 1.59 μM) and neuronal (IC_{50} = 8.7 μM for $\alpha3\beta4$) and neuromuscular (IC_{50} = 0.54 μM for $\alpha1\beta1\epsilon\delta$) subtypes of the nicotinic acetylcholine receptor (nAChR). Similarities in sequence and structure are apparent between the middle loop of pl14a and the second loop of a number of α-conotoxins. This is the first conotoxin shown to affect the activity of both voltage-gated and ligand-gated ion channels.

Cone snails are predatory marine gastropods that belong to the genus *Conus;* different species prey on fish, other molluscs, or worms. The ability of the fish-hunting cone snails to capture prey successfully is based on the combined action of neuroactive peptides (*1*) injected into the fish. Most characterized cone snail toxins have been isolated from the venom of piscivorous cones (*2*, *3*). The identification of specific receptor targets for these conotoxins has facilitated our understanding of molecular mechanisms, which underlie the rapid fish immobilization that occurs with envenomation (*1*, *4*).

The vermivorous *Conus* species comprise the largest group of cone snails; they feed on various types of marine worms, including different polychaetes (*5*, *6*). There are greater than 4 times more worm-hunting *Conus* species than piscivorous species. The great variety of marine worm species found in different marine environments provides the basis for the worm-feeding cones to develop different hunting strategies and evolve neuroactive venom components that are optimized for specific types of marine worms. Several conotoxins have been identified in the venoms of worm-feeding cones (*7*−*17*), but the mechanisms of envenomation of prey by the vermivorous *Conus* species are not well characterized.

Conopeptides are the active peptidic components in cone snail venoms, and these are classified into two major groups. One group consists of disulfide-rich peptides commonly termed conotoxins; the second group comprises peptides with only one disulfide bond or none. The cysteine-rich conotoxins are encoded by gene superfamilies that share significant sequence similarity. Conotoxins that belong to the same gene superfamily share a characteristic disulfide pattern and a general pharmacological targeting specificity (*18*).

This paper describes the identification and characterization of a conotoxin from the vermivorous cone *Conus planorbis* (Figure 1). *C. planorbis* is commonly found in the Indo-Pacific region and belongs to Clade IX in the phylogenetic scheme for *Conus* of Espiritu et al. (*19*), equivalent to E5 of Duda et al. (*5*). The new peptide, which we call conotoxin pl14a, is active in the mammalian nervous system. It inhibits the Kv1.6 subtype of the voltage-gated K^+ channel and some

[†] This work was supported by the National Institutes of Health (Grant GM48667 to B.M.O.), the German Ministry of Education and Research Biofuture Prize (Förderkennzeichen 0311859 to H.T.), and the Australian Research Council (P.F.A. and D.J.C.).

[‡] The coordinates for pl14a have been deposited as PDB entry 2FQC. The following GenBank nucleotide accession numbers have been deposited: DQ447640 for pl14a, DQ447641 for pl14.1, DQ447642 for pl14.2, DQ447643 for pl14.3, DQ447644 for fe14.1, and DQ447645 for fe14.2.

* To whom correspondence should be addressed: Department of Biology, University of Utah, 257 S. 1400 E., Salt Lake City, UT 84112. Telephone: (801) 581-5907. Fax: (801) 585-5010. E-mail: imperial@biology.utah.edu.

[§] University of Utah.

[||] The University of Queensland.

[⊥] Max-Planck-Institute for Experimental Medicine.

[@] Universitaetsklinikum Schleswig-Holstein.

10.1021/bi060263r CCC: $33.50
Published on Web 06/16/2006

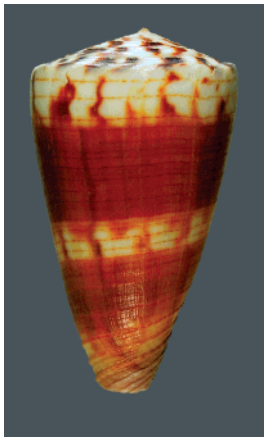

FIGURE 1: A 5 cm long *C. planorbis* shell.

nicotinic acetylcholine receptor (nAChR)[1] subtypes. pl14a defines a new gene superfamily of conotoxins, the J-conotoxin superfamily.

MATERIALS AND METHODS

Isolation of pl14a from C. planorbis Venom. Snails were collected in the Marinduque Islands, Philippines, and dissected. Venom was pressed out of the venom ducts, and the venom pooled from several snails was lyophilized and stored at −70 °C. A 500 mg portion was resuspended in 35 mL of 30% acetonitrile and 0.2% trifluoroacetic acid (TFA) using a vortex mixer for 2 × 1 min with an interval of 5 min on ice. The mixture was sonicated using a Branson LS-75 probe for 3 × 0.5 min on ice with 1 min rest periods, and the sediment was pelleted in a Beckman Avanti centrifuge with an F650 rotor for 30 min at 37500*g*. The supernatant was diluted with 0.1% TFA, centrifuged again to remove all residual particles, and applied to a preparative Vydac C_{18} high-pressure liquid chromatography (HPLC) column (2.5 cm × 25 cm). Venom peptides were eluted from the column with a linear gradient from 4.5 to 90% acetonitrile with 0.1% TFA at 0.9% acetonitrile/min. The flow rate was 20 mL/min, and the absorbance of the eluate was monitored at 220 nm. An analytical Vydac C_{18} HPLC column (4.6 mm × 250 mm) with linear gradients at 0.18 or 0.09% acetonitrile/min in 0.1% TFA was used for subsequent fractionations. The flow rate was 1 mL/min, and absorbance at 220 and 280 nm was monitored.

pl14a Synthesis. Linear p114a was assembled on a Boc-phe-pam resin as previously described (*20*). A Boc-amide linker (*21*) and Boc-amino acids were preactivated with an equivalent amount of 2-(1*H*-benzotriazol-1-yl)-1,1,3,3-tetramethyluronium hexafluorophosphate in the presence of diisopropylethylamine. Each coupling was monitored by the ninhydrin reaction except coupling to proline, which was monitored by the isatin test. HF cleavage was carried out at 5 °C for 1.5 h.

The crude linear peptide was purified by HPLC on a semipreparative C_{18} column (1 cm × 25 cm) with an elution gradient of 0.9% acetonitrile/min in 0.1% TFA. Folding was achieved by air oxidation at a peptide concentration of 0.1−0.2 mM in 0.1 M ammonium bicarbonate (pH 8) for 20 h. Coelution with native pl14a was demonstrated using an analytical C_{18} HPLC column with a linear gradient of 0.45 or 0.18% acetonitrile/min in 0.1% TFA. The flow rate was 1 mL/min in a Waters Millennium HPLC system with auto sampler.

Characterization of Peptides. Mass determinations on both native and synthetic peptides were accomplished by matrix-assisted laser desorption ionization (MALDI), or electrospray ionization (ESI) mass spectrometry (MS) at the University of Utah Mass Spectrometry and Proteomic Core Facility, the Salk Institute Peptide Biology Lab, and The University of Queensland Institute for Molecular Bioscience. The amidation of the C-terminus was shown on the native peptide from mass values obtained by ESI-MS.

The disulfide bond connectivity was determined using the partial reduction and alkylation procedure as described previously (*22*). Partial reduction was achieved in the presence of 10 mM tris(2-carboxyethyl)phosphine hydrochloride (TCEP-HCl) in 0.085 M sodium citrate, 0.05% TFA, and 14% acetonitrile (pH 3) for 20 min at 23 °C. The products were separated by HPLC, and the putative reduced peaks were alkylated using iodoacetamide. The alkylation reaction mixtures were fractionated by HPLC, and the partially alkylated product was identified by mass spectrometry. Alkylation after complete reduction with 10 mM dithiothreitol was done using 0.7% 4-vinylpyridine. The sequences of partially and fully alkylated peptides were determined by R. Schackmann, using Edman degradation chemistry in an Applied Biosystems model 477A protein sequencer at the Protein/DNA Core Facility of the University of Utah Huntsman Cancer Institute.

NMR Spectroscopy and Structure Calculations. Samples for ^{1}H NMR measurements contained ∼1 mM peptide in a 95% H_2O/5% D_2O mixture (v/v) at pH ∼3. Spectra were recorded at 290 K on a Bruker Avance-600 spectrometer equipped with a shielded gradient unit. Two-dimensional NMR spectra were recorded in phase-sensitive mode using time-proportional phase incrementation for quadrature detection in the t_1 dimension as previously described for other disulfide-rich peptides (*23*, *24*). $^3J_{HN-H\alpha}$ coupling constants were measured from a one-dimensional spectrum or from the DQF-COSY spectrum.

Spectra were processed on a Silicon Graphics Indigo workstation using XWINNMR (Bruker) software. The t_1 dimension was zero-filled to 1024 real data points, and 90° phase-shifted sine bell window functions were applied prior to Fourier transformation. Chemical shifts were referenced to internal 2,2-dimethyl-2-silapentane-5-sulfonate.

Preliminary structures of pl14a were calculated using a torsion angle simulated annealing protocol within DYANA (*25*). Final structures were calculated using CNS version 1.1 (*26*). A set of 50 structures was generated by a torsion angle simulated annealing protocol as previously described (*23*, *24*). Structures were analyzed using PROMOTIF (*27*) and PROCHECK-NMR (*28*).

Cloning. Total RNA preparations from a single duct each of *C. planorbis* (Figure 1) and *Conus ferrugineus* were obtained using the Qiagen RNeasy mini protocol for isolation of total RNA from animal tissues. Each RNA preparation (4.5 μg for *C. planorbis* and 5.1 μg for *C. ferrugineus*) was

[1] Abbreviations: nAChR, nicotinic acetylcholine receptor; TFA, trifluoroacetic acid; MALDI, matrix-assisted laser desorption ionization; ESI, electrospray ionization; UTR, untranslated region; RACE, rapid amplification of cDNA ends; ACh, acetylcholine; SAR, structure−activity relationship.

used in cDNA synthesis (*29*). The 3′-untranslated region (UTR) for pl14a was identified by synthesizing degenerate oligonucleotide primers designed from the carboxy-terminal regions of the peptide, and the primers were used in a 3′-rapid amplification of cDNA ends (RACE) (*29*). Another oligonucleotide primer was designed from the identified 3′-UTR and used in a 5′-RACE using the Clonetech SMART RACE kit and protocol.

Oligonucleotide primers derived from the 3′-UTR and 5′-prepropeptide regions of the pl14a clone were used to screen the cDNAs described above for more clones in the J-superfamily. All PCR runs were done in a Peltier Thermal Cycler 2000 instrument using Invitrogen High Fidelity Platinum Taq DNA polymerase. The Invitrogen TA cloning kit was used for all transformations. DNA sequencing was carried out at the University of Utah Huntsman Cancer Institute Protein/DNA Core Facility using samples prepared following the Qiagen mini prep kit protocol.

The sequences of all oligonucleotide primers derived from the native peptide or clones are included as Supporting Information.

Biological Assays. Intracranial injections were administered to mice that were 15−17 days old. Peptide samples were resuspended in 12 μL of normal saline solution and administered to the mice using an insulin syringe. The peptide-injected mice were observed side by side with saline-injected controls continuously for 2−4 h and checked the next day.

nAChR Assay. Recordings were made from *Xenopus* oocytes expressing mouse skeletal muscle nAChR subtypes and rat neuronal subtypes, in a static bath of ND-96 solution as previously described (*30*). Oocytes were injected 1−2 days after harvesting and used for voltage clamp recording 3−8 days after injection. The bath contained bovine serum albumin at a concentration of 0.1 mg/mL to minimize nonspecific adsorption of the toxin and atropine at 1 μM to block endogenous muscarinic acetylcholine receptors. Acetylcholine (ACh)-gated currents were elicited with 1−10 μM ACh for oocytes expressing the muscle skeletal subtypes and 100 μM ACh for oocytes expressing the neuronal subtypes. The toxin was allowed to equilibrate in the static bath for 5 min prior to pulsing with ACh by gravity perfusion.

Three oocytes were used for each data point. Dose−response curves were fit to the equation % response + 100/[1 + (toxin concentration/IC_{50})n_H], where n_H is the Hill coefficient.

K^+ Channel Assays. The *Xenopus* oocyte expression system was used to study the effect of pl14a on Kv1 channels. Oocytes were treated, and Kv1 channels were expressed as described previously (*31*). Whole-cell currents were recorded under two-electrode voltage-clamp control using a Turbo-Tec amplifier (npi electronic, Tamm, Germany). Current records were low-pass-filtered at 1 kHz (−3 db) and sampled at 4 kHz. The bath solution was normal frog Ringer's solution (*32*) containing 115 mM NaCl, 2.5 mM KCl, 1.8 mM $CaCl_2$, and 10 mM Hepes (pH 7.2) (NaOH). All electrophysiological experiments were performed at room temperature (19−22 °C).

The IC_{50} values for the block of the Kv1.6 channel were calculated from the peak currents at a test potential of 0 mV according to the equation IC_{50} = fc/(1 − fc) × [Tx], where fc is the fractional current and [Tx] is the toxin concentration.

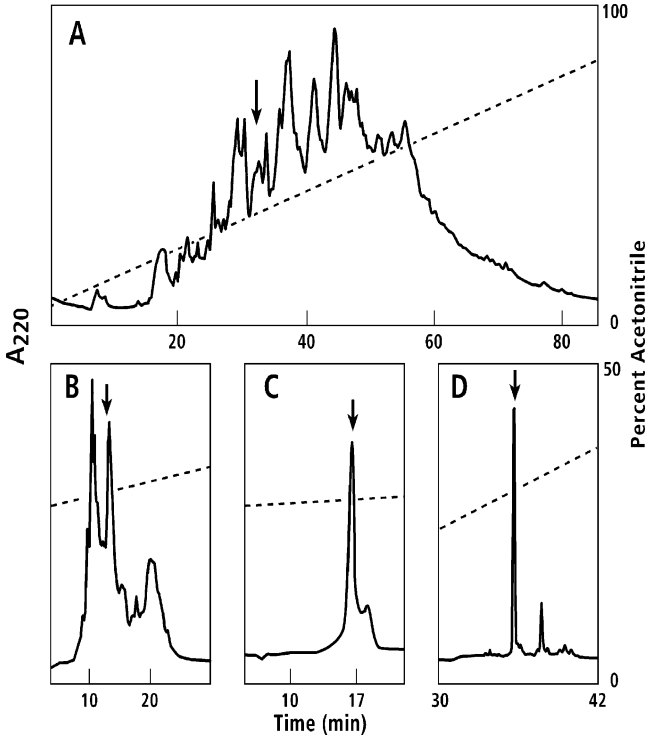

FIGURE 2: Isolation of pl14a from *C. planorbis* venom. The arrow in each HPLC run indicates the location of the fraction containing the peptide. All the elution buffers had 0.1% TFA. (A) The venom extract was chromatographed in a preparative Vydac C_{18} column eluted with 4.5 to 90% acetonitrile. (B) The peak containing the peptide in A was subfractionated using an analytical Vydac C_{18} column and an elution gradient of 28 to 34% acetonitrile. (C) The fraction containing the peptide in B was further subfractionated using a gradient of 0.09% acetonitrile/min. (D) The major peak in C was completely reduced and alkylated and then chromatographed in an analytical Vydac C_{18} column eluted with a gradient of 0.9% acetonitrile/min. The major peak yielded the sequence for pl14a.

Tests on *Xenopus* oocytes expressing Kv2.1 and Kv3.4 channels were done under similar conditions.

Other Activity Assays. The activity of pl14a was also tested in *Xenopus* oocytes expressing the Nav1.2 channel, under conditions similar to those used in the K^+ channel assays.

The effect of pl14a on the binding of [^{125}I]GVIA to rat synaptosomes was tested using the membrane filtration assay (*33*).

RESULTS

Isolation and Structural Characterization of pl14a. An initial fractionation of *C. planorbis* venom was carried out to isolate and characterize major venom components. To identify conotoxin-like components, major components within the 2−4 kDa range were completely reduced and alkylated. The number of disulfide bonds in specific peptides within the mass range given above was obtained by mass spectrometry of samples before and after complete reduction and alkylation.

The chromatograms in Figure 2 show the HPLC separation of the venom components of *C. planorbis* and the isolation of pl14a. The complete reduction and alkylation of the peak indicated in Figure 2C suggested the presence of four cysteines. However, the MALDI and ESI average mass of 2911 Da for this conopeptide was approximately double the mass of peptides in known conotoxin superfamilies (A and

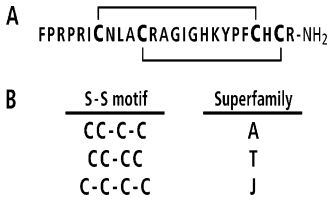

FIGURE 3: (A) Peptide sequence of pl14a showing the disulfide connectivity. (B) Disulfide motifs found in conotoxin superfamilies with four cysteines.

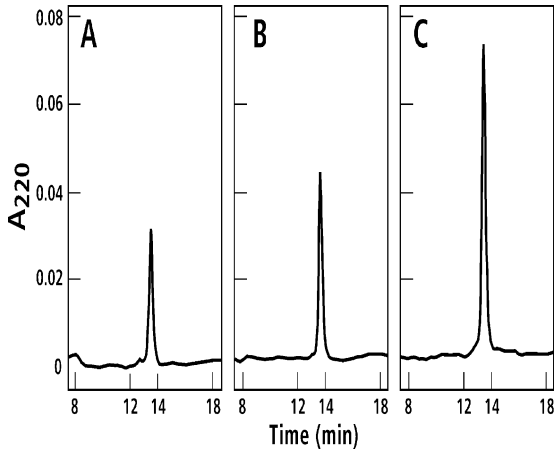

FIGURE 4: Coelution of native and synthetic preparations of pl14a. The HPLC runs were carried out using a gradient of 0.45% acetonitrile/min in 0.1% TFA: (A) pl14a isolated from *C. planorbis* venom, (B) synthetic pl14a, and (C) a mixture of the native and synthetic samples of pl14a identical to those used in the individual runs.

T) with a four-cysteine pattern (*18*). Sequencing showed that the peptide has a cysteine pattern different from those in the previously characterized four-cysteine superfamilies (Figure 3). The ESI monoisotopic mass value of 2909.5 Da for the native peptide indicated an amidated C-terminus. This peptide is initially called pl14a, based on the species name (*C. planorbis*) followed by the number representing the 14th cysteine pattern found in conotoxins (*16*), with the letter "a" representing the first peptide characterized in this class from *C. planorbis*. As we will demonstrate below, the peptide defines a new superfamily of conotoxins, which we call the J-conotoxin superfamily.

Peptide Synthesis and Determination of Disulfide Connectivity. pl14a was chemically synthesized as described in Materials and Methods. Panels A−C of Figure 4 show the HPLC chromatograms of the sample isolated from the venom, the predominant form obtained after overnight air oxidation at pH 8, and the coelution of both, respectively, which indicates that the folded synthetic preparation of pl14a is identical to the peptide present in the venom. A yield of 0.45 mg of pl14a was typically obtained from 1 mg of linear peptide.

Panels A and B of Figure 5 show the HPLC profiles of the partial reduction and alkylation reactions, respectively. The partially reduced pl14a overlaps with the native folded peptide but can be completely separated from it after partial alkylation with iodoacetamide (*22*). Sequencing of both the partially alkylated peptide and of the peptide with pyridylethylation of the second pair of cysteines showed a 1−3, 2−4 disulfide connectivity (Figure 3).

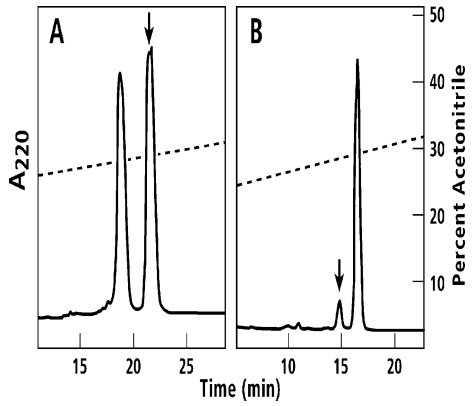

FIGURE 5: Partial reduction and alkylation of pl14a. (A) The HPLC chromatogram after partial reduction shows the peak of the peptide with one disulfide bond cleaved (indicated by arrow) overlapping with the peak of the native peptide. The adjacent peak is that of the completely reduced pl14a. (B) The HPLC profile of the alkylation reaction shows the separation of the partially alkylated p14a (indicated by arrow) from the native peptide.

Table 1: NMR and Refinement Statistics for pl14a

NMR distance and dihedral constraints	
distance constraints	
total NOE	178
sequential ($\|i-j\|=1$)	93
medium-range ($\|i-j\|<5$)	54
long-range ($\|i-j\|>5$)	31
total dihedral angle restraints	
ϕ	15
χ_1	4
structure statistics	
violations (mean ± standard deviation)	
distance constraints (Å)	0.035 ± 0.003
dihedral angle constraints (deg)	0.25 ± 0.2
maximum dihedral angle violations (deg)	3
maximum distance constraint violations (Å)	0.3
deviations from idealized geometry	
bond lengths (Å)	0.003 ± 0.0002
bond angles (deg)	0.46 ± 0.02
impropers (deg)	0.31 ± 0.02
average pairwise rmsd[a] (Å)	
heavy atoms (residues 7−23)	0.16 ± 0.06
backbone atoms (residues 7−23)	1.50 ± 0.26
Ramachandran statistics (residues 3−24)	
most favored	80.6%
additionally allowed	19.4%

[a] The pairwise rmsd was calculated among 20 refined structures.

Solution Structure of pl14a. NMR spectral assignments for pl14a were made using established techniques (*34*); the ^{1}H chemical shifts are supplied as Supporting Information. The chemical shifts in the amide region are well-dispersed, and the large number of resolved cross-peaks in the NOESY spectrum allowed determination of a well-defined structure for the majority of the molecule.

The three-dimensional structure of pl14a was calculated with 178 distance restraints and 19 angle restraints using a simulated annealing protocol in CNS. Ten restraints for five hydrogen bonds were included, based on the slowly exchanging amide protons and preliminary structures. The resulting family of structures had good structural and energetic statistics, as shown in Table 1. An ensemble and ribbon representation of the three-dimensional structure is shown in Figure 6. Analysis of the structures with PROMOTIF (*27*) identified an α-helical region between residues

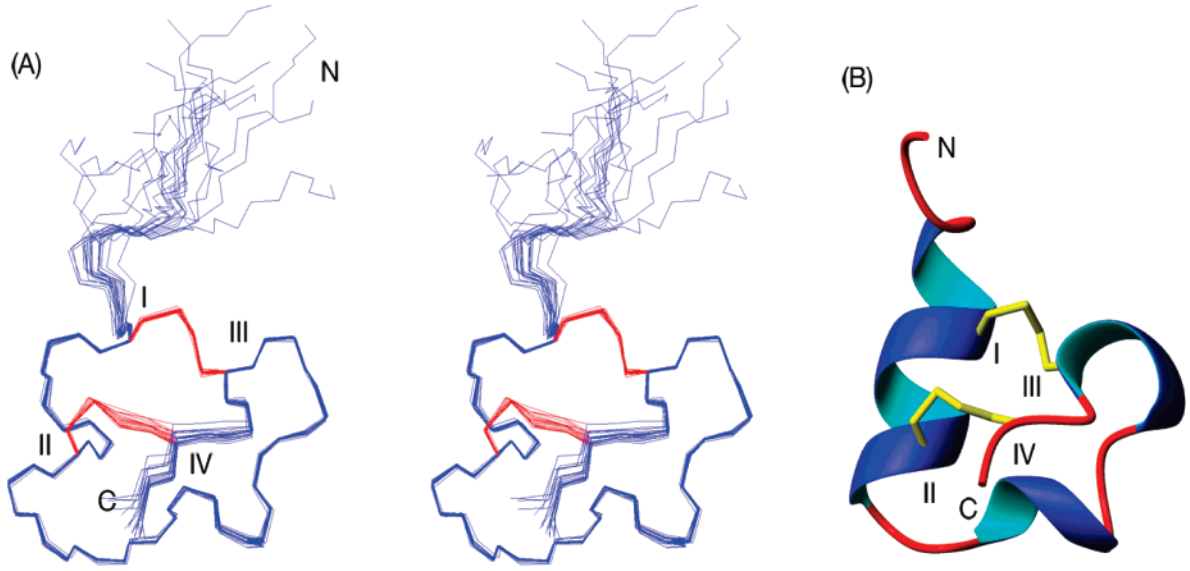

FIGURE 6: Three-dimensional structure of pl14a. (A) A superposition of the 20 lowest-energy structures of pl14a. (B) A ribbon representation of the secondary structure of pl14a.

A

ATG CCG TCT GTT CGG TCT GTG ACC TGC TGC TGT CTG CTG TGG ATG
M P S V R S V T C C C L L W M

↓1
ATG TTC TCT GTA CAG CTC GTC ACT CCT GGC TCC CCT GGA ACT GCA
M F S V Q L V T P G S P G T A

↓2
CAG CTG TCT GGG CAT CGC ACT GCT AGA TTT CCT AGA CCG AGA ATA
Q L S G H R T A R F P R P R I

TGC AAT CTG GCG TGC AGG GCG GGA ATC GGA CAC AAG TAT CCC TTT
C N L A C R A G I G H K Y P F

Mature Peptide

↓3
TGC CAT TGC AGA GGG AAA CGG
C H C R G K R

B

pl14a	FPRPRICNLACRAGIGHKYPFCHCR–NH_2
pl14.1	GPGSAICNMACRLGQGHMYPFCNCN–NH_2
pl14.2	GPGSAICNMACRLEHGHLYPFCHCR–NH_2
pl14.3	GPGSAICNMACRLEHGHLYPFCNCD–NH_2
fe14.1	SPGSTICKMACRTGNGHKYPFCNCR–NH_2
fe14.2	SSGSTVCKMMCRLGYGHLYPSCGCR–NH_2

FIGURE 7: (A) pl14a clone. The arrows indicate the predicted cleavage sites between the signal sequence and the propeptide (arrow 1) using SignalP 3.0 Server and between the propeptide and the mature pl14a (arrow 2). (B) Homologous sequences identified from the cDNA of *C. planorbis* and *C. ferrugineus*.

6 and 12 and 3_{10}-helices between residues 15−17 and 20−22.

pl14a Clone. Figure 7A shows the precursor sequence of pl14a. The only post-translational processing occurring in this peptide, which is C-terminal amidation, is demonstrated by the sequence ...RGKR at cleavage site 3 in Figure 7A (*35*) which results in the amidation of the C-terminal R of the mature peptide. The unique signal sequence, MPSVRS-VTCCCLLWMMFSVQLVTP, indicates that p14a is the first peptide in a new superfamily of conotoxins that we have termed the J-superfamily. Using oligonucleotide primers from the signal sequence and the 3′-UTR, additional members of the J-superfamily were identified (Figure 7B) from *C. planorbis* and *C. ferrugineus* (Figure 1), a species that also belongs to Clade IX. The peptide length, the loop sizes, and the C-terminal amidation are maintained among the peptides identified, so far. Residues R^{12}, G^{16}, H^{17}, Y^{19}, and P^{20} are conserved, and there is a conservative substitution of valine for I^6.

Biological Activity of pl14a in Mice. Behavioral symptoms were elicited upon intracranial injection of the synthetic peptide in mice, indicating that this targets the mammalian central nervous system. At an average dose of 0.5 nmol/g of mouse body weight, the symptoms included rapid circling and shaking, with the shaking occurring when the mouse moved or attempted to move. These symptoms started as early as a few minutes after injection and lasted for an average of one to a few hours. At double the dose, the rapid circling and/or shaking symptoms were still observed in most cases, but more severe symptoms such as barrel rolling and seizures were common. Further doubling the dose resulted in death in at least 50% of the injected mice. Intraperitoneal injections at levels similar to those used in intracranial injections did not produce any apparent symptom in the mice.

Intramuscular injection in goldfish and injection at the anterior end of a marine polychaete (*Nereis virens*), likewise, did not give any definitive symptomatology.

Activity in Nicotinic Acetylcholine Receptor Assays. The synthetic pl14a was tested for activity in neuronal and muscle subtypes of nAChR expressed in oocytes. Initial tests were carried out at 10 μM, and in the muscle subtypes of the nAChR, the peptide was approximately 50% more active in the adult mouse subtype ($\alpha1\beta1\epsilon\delta$) than in the fetal form ($\alpha1\beta1\gamma\delta$). The dose−response plot of the pl14a activity in $\alpha1\beta1\epsilon\delta$ (Figure 8) gave an IC_{50} of 0.54 μM (95% confidence interval: 0.50−0.57 μM). Figure 8 also shows the dose−response plot of the activity in the $\alpha3\beta4$ subtype of the rat neuronal nAChR, which gave the highest activity among eight neuronal forms that were tested (Supporting Information), and the IC_{50} obtained was 8.7 μM (95% confidence interval: 7.3−10.4 μM).

Activity in K^+ Channel Assays. To investigate a potential interaction of pl14a with voltage-activated K^+ channels, different isoforms in the Kv1 subfamily (Kv1.1−Kv1.6) were

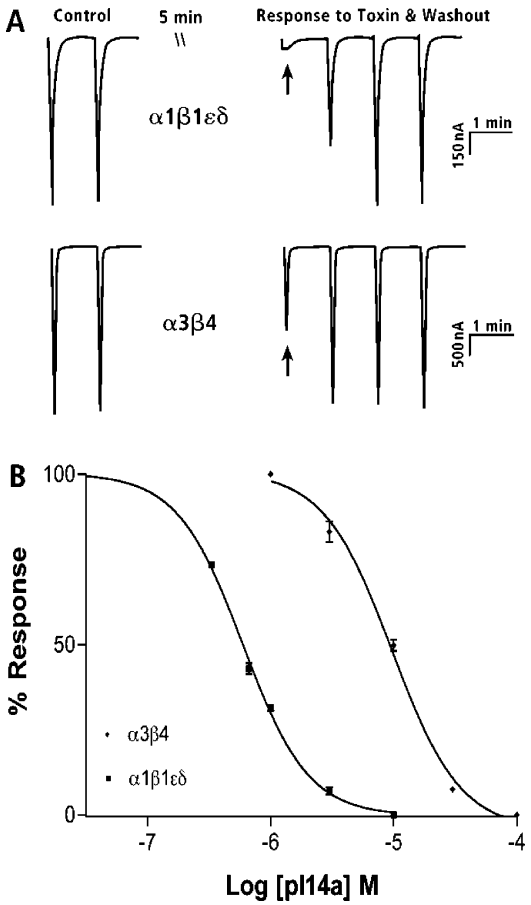

FIGURE 8: Activity of pl14a in nAChR assays. (A) pl14a was applied to oocytes expressing the nAChR subtypes at 3 μM for the muscle subtype ($\alpha1\beta1\epsilon\delta$) and at 10 μM for the neuronal subtype ($\alpha3\beta4$). Arrows indicate the first currents elicited after toxin equilibration for 5 min, by an ACh pulse of 1−10 μM for the muscle skeletal subtypes and 100 μM for the neuronal subtypes. pl14a at 3 μM blocked the elicited currents nearly completely in $\alpha1\beta1\epsilon\delta$, and the toxin dissociated rapidly from the receptor. A block of approximately 50% of the elicited current was obtained in $\alpha3\beta4$, with a similar dissociation rate. (B) Dose−response curves for pl14a in each subtype. Each data point is the average of responses obtained from three oocytes, and the curves were generated using Prism. The IC_{50} for the adult mouse muscle subtype is 0.54 μM, and the IC_{50} for the rat $\alpha3\beta4$ neuronal subtype is 8.7 μM.

expressed in *Xenopus* oocytes, and potential changes for the evoked currents in the presence of 1 μM pl14a were measured. At this concentration, a very small blocking effect was observed for Kv1.1, and no effect was observed for Kv1.2−Kv1.5 (see Figure 9). In contrast, a profound block of the currents was observed for Kv1.6. The IC_{50} for the block was 1.59 ± 0.96 μM (mean ± the standard deviation; $n = 8$).

pl14a was also assayed in *Xenopus* oocytes expressing Kv2.1 and Kv3.4 channels. No inhibition of the evoked response was observed in these channels at 2 μM pl14a (data not shown).

Other Activity Assays. The addition of 2 μM pl14a to *Xenopus* oocytes expressing the Nav1.2 channel also showed no effect on the evoked response, indicating that pl14a does not affect these Na currents.

The presence of 5 μM pl14a in an ω-GVIA membrane binding assay (*33*) did not displace any binding of [^{125}I]GVIA to rat synaptosomes (data not shown). This result implies that pl14a does not bind to N-type presynaptic Ca^{2+} channels.

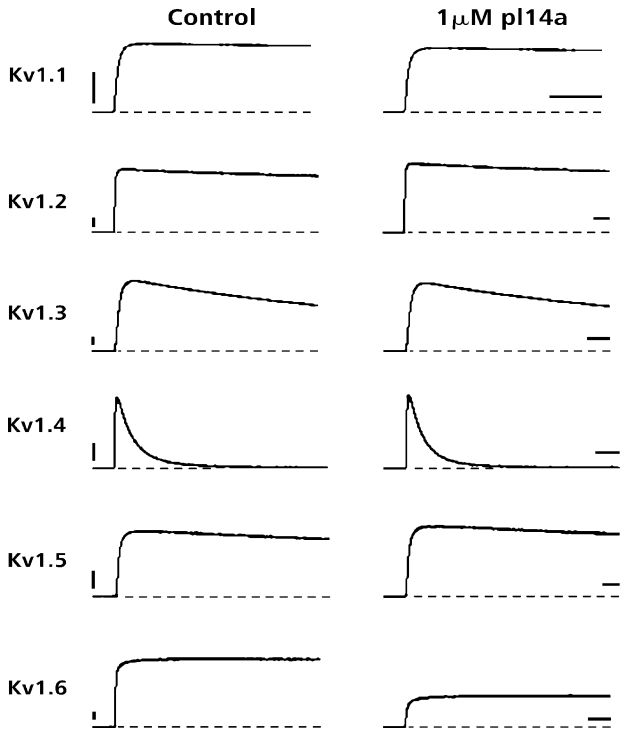

FIGURE 9: pl14a blocks Kv1.6 channels. (Left) Whole-cell currents obtained for depolarizing pulses to 0 mV from a holding potential of −100 mV from oocytes expressing different Kv1 channels. The bath solution was normal frog Ringer's solution. (Right) Addition of 1 μM pl14a had almost no effect for Kv1.1−Kv1.5-mediated currrents, whereas Kv1.6-mediated currents are blocked by ~50%. The horizontal bars correspond to 50 ms and the vertical bars to 1 μA. Current records were low-pass-filtered at 1 kHz (−3 db) and sampled at 4 kHz.

DISCUSSION

We isolated and characterized a conotoxin from the Indo-Pacific worm-hunting cone *C. planorbis*, designated pl14a, which is 25 amino acid residues long with a $X_6CX_3CX_{10}$-CXCX cysteine pattern (Figure 3). The only post-translational modification present in the peptide is amidation of the C-terminus, which was detected from the monoisotopic ESI mass value and confirmed by the presence of a standard amidation sequence of a peptidylglycine after proteolytic cleavage of the precursor peptide (Figure 7A) (*35*). The disulfide connectivity was determined by stepwise reduction and alkylation and confirmed by the NMR solution structure (Figure 6) to be C^1-C^3 and C^2-C^4, as shown in Figure 3.

The cloning data provided evidence that the peptide we characterized from *C. planorbis* venom, conotoxin pl14a, belongs to a new gene superfamily, the J-conotoxin superfamily. Five homologous peptides (Figure 7B) were identified in the cDNA prepared from the venom ducts of *C. planorbis* and the closely related species *C. ferrugineus*, using oligonucleotide primers derived from the signal sequence and the 3′-UTR of the p14a clone (Figure 7A). It is notable that the peptides identified from these vermivorous species are identical in length and loop sizes to pl14a, and all are C-terminally amidated.

A recent report of a series of peptides from worm-hunting Western Atlantic cone species (*16*) showed that peptides with a C-C-C-C cysteine pattern may be common components of venoms of vermivorous cones. Furthermore, the loop sizes

Table 2: Conotoxins with the 14th Cysteine Framework (C-C-C-C)

Name	Primary Structure	Disulfide Connectivity	Snail species	Reference
pl14a	FPRPRI**C**NLA**C**RAGIGHKYPF**C**H**C**R*	C1-C3,C2-C4	*C. planorbis*	this work
pl14.1	GPGSAI**C**NMA**C**RLGQGHMYPF**C**N**C**N*	---	*C. planorbis*	this work
pl14.2	GPGSAI**C**NMA**C**RLEHGHLYPF**C**H**C**R*	---	*C. planorbis*	this work
pl14.3	GPGSAI**C**NMA**C**RLEHGHLYPF**C**N**C**D*	---	*C. planorbis*	this work
fe14.1	SPGSTI**C**KMA**C**RTGNGHKYPF**C**N**C**R*	---	*C. ferrugineus*	this work
fe14.2	SSGSTV**C**KMM**C**RLGYGHLYPS**C**G**C**R*	---	*C. ferrugineus*	this work
---	KFLSGGFKγIV**C**HRY**C**AKGIAKEF**C**N**C**PD	---	*C. geographus*	(*36*)
flfl4a	WDVND**C**IHF**C**LIGVVERSYTE**C**HTM**C**T	C1-C4,C2-C3	*C. floridanus floridensis*	(*16*)
flf14b	WDVND**C**IHF**C**LIGVVGRSYTE**C**HTM**C**T	C1-C4,C2-C3	C. *floridanus floridensis*	(*16*)
flf14c	WDAYD**C**IQF**C**MRPEMRHTYAQ**C**LSI**C**T	C1-C4,C2-C3	*C. floridanus floridensis*	(*16*)
vil14a	GGLGR**C**IYN**C**MNSGGGLSFIQ**C**KTM**C**Y	C1-C4,C2-C3	*C. villepinii*	(*16*)

*An amidated C-terminus.

Table 3: Sequence Homologies between pl14a and α-Conotoxin Blockers of nAChR

Name	Primary Structure	IC_{50} in muscle subtype (nM)	IC_{50} in $\alpha3\beta4$ (nM)	Reference
α-MI	GRCCHPAC**GKNY**SC-NH_2	12.0 ($\alpha1\beta1\gamma\delta$)		(*50*)
α-GI	ECCNPAC**GRHY**SC-NH_2	20.0 ($\alpha1\beta1\gamma\delta$)		(*50*)
α-SI	ICCNPAC**GPKY**SC-NH_2	170 ($\alpha1\beta1\gamma\delta$)		(*37*)
p114a	FPRPRICNLACRAGI**GHKY**PFCHCR-NH_2	540 ($\alpha1\beta1\varepsilon\delta$)	8700	this work
α-AuIB	GCCSYPPCFATNPDC-NH_2		750	(*51*)
α-PeIA	GCCSHPACSVNHPELC-NH_2		480	(*52*)
α-BuIA	GCCSTPPCAVLYC-NH_2		27.7	(*53*)

could be variable, as well as the disulfide connectivity. Table 2 compares all known peptide sequences with the 14th cysteine pattern that have been reported to date. The peptide from the venom of the piscivorous species *Conus geographus* (*36*) shows that this cysteine pattern is also present in the venoms of piscivorous species. The question of whether all of the peptides in Table 2 belong to the J-superfamily remains. The screening of cDNA derived from other *Conus* species for J-superfamily peptides is ongoing.

The three-dimensional structure of pl14a (Figure 6) represents a novel structural fold and is well-defined, with the exception of the N-terminal region. This disorder is likely to be from structural flexibility, as there are no disulfide bonds in the N-terminal region to constrain the molecule. The major element of secondary structure is an α-helix between residues 6 and 12. Both disulfide bonds (7−22 and 11−24) have one half-cystine located in this helical region, and formation of the disulfide bonds results in a compact three-dimensional structure. Although the disulfide connectivity of pl14a is the same as that of the α-conotoxins (i.e., C^1-C^3, C^2-C^4), the secondary structure and the position of the C-terminus are not conserved. Despite these differences, there are structural similarities between the backbone conformation for residues 11−21 in pl14a and the conformation observed for residues 4−12 in α-conotoxin SI. As the α-conotoxins are antagonists of the nAChR and possess a common structural motif, the similarities between pl14a and α-conotoxin SI may be relevant to the activity of pl14a observed at the nAChR.

Table 3 shows an alignment of the sequence of pl14a with those of some α-conotoxins. The lower IC_{50} observed for pl14a on the adult muscle nAChR subtype over the neuronal ones is consistent with the degree of sequence similarity between pl14a and the α-conotoxins that block the muscle subtype, being greater than that shown with known blockers for the neuronal subtype $\alpha3\beta4$. In a SAR study on the residues in α-GI and in α-SI that are critical to the binding to nAChRs in mouse muscle-derived BC_3H-1 cells and *Torpedo* (*37*), it was shown that residues 9 and 10 were involved in the interaction of these conotoxins with the receptor. The corresponding residues in pl14a (residues 17 and 18, respectively) and the adjacent ones (highlighted residues) are closely related, if not identical, to those in the α-conotoxins. The fact that the potency of pl14a is much lower than that of GI or SI could be due to subtle changes in the secondary structure that is presented.

A number of diverse conotoxins were previously shown to affect other K^+ channels. These include the κ- (*38*) and κM-conotoxins (*39*) and the conkunitzins (*40*, *41*), all from fish-hunting *Conus* species. To our knowledge, this is the first report of a peptide that selectively inhibits the Kv1.6 channel activity among the different Kv1 forms. A very diverse group of peptides identified in animal toxins have been found to block Kv1 channel subtypes (*42*−*45*). A phylogenetic tree was generated from some of these toxins and is shown in Figure 10. The conotoxins form two different branches from the rest of the toxins from scorpion and sea anemone. All J-superfamily peptides are in one branch and

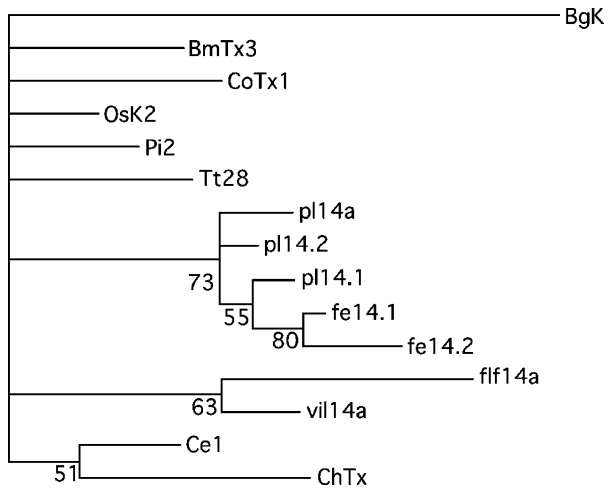

FIGURE 10: Phylogenetic tree (Bayesian estimate at 50% majority rule) of conotoxins in the J-superfamily, pl14a, pl14.1, pl14.2, pl14.3, fe14.1, and fe14.2 (this paper), other conotoxins with the same cysteine pattern, flf14a and vil14a (*16*), and other Kv1 channel toxins, which include BgK (*42*) from sea anemone and Ce1 (*54*), ChTx (*55*), CoTx1 (*56*), OsK2 (*57*), Pi2 (*58*), and Tt28 (*59*) from scorpion. Scorpion toxin BmTx3 blocks both A-type K^+ and HERG currents (*60*).

separate from the other conotoxins with the same cysteine framework but with a different three-dimensional structure.

Two types of structural features are shared and have been proposed to play a role in the activity on Kv1 channels. The first is a dyad structure, made up of a positively charged (usually lysine) and a hydrophobic amino acid (usually aromatic), protruding from a relatively flat surface made up of the other amino acid residues of the peptide. The lysine α-carbon and the center of the aromatic ring are within 6−7 Å of each other (*45*, *46*), with the lysine residue occluding the K^+ channel pore (*47*). In some Kv1 channel inhibitors without the functional dyad, the presence of a ring of basic residues on one surface of the molecule has been demonstrated to play a role in the binding of a peptide to the outer vestibule of the channel (*48*, *49*). There is both a potential dyad as well as a ring of basic residues in pl14a; one or both of these structural elements may be important for the interaction of the peptide with the Kv1.6 channel.

The demonstration of the activity of pl14a on both the Kv1.6 channel and in nAChR subtypes is the first observation of a *Conus* peptide inhibiting both a voltage-gated and a ligand-gated ion channel. The symptomatology observed in mice treated with the peptide suggests that the K^+ channel activity is the dominant effect in mammals *in vivo*. The role of specific residues in the peptide that may affect either or both of these activities is currently being examined via chemical syntheses and functional evaluation of alanine-substituted analogues.

ACKNOWLEDGMENT

We thank Dr. Michael Ellison and Dr. James Garrett for helpful suggestions on the RACE procedure and Dr. Aryan Azimi-Zonooz for the ω-GVIA binding assay. We also thank John-Paul Ownby for assistance with software, Kerry Matz for preparation of figures, and Sean Christensen for oocyte preparation. The work of J.S.I. was done at the University of Utah and the Institute for Molecular Bioscience, The University of Queensland, in partial fulfillment of requirements for a research Ph.D. with the Department of Biochemistry and Molecular Biology, School of Molecular and Microbial Sciences, The University of Queensland.

SUPPORTING INFORMATION AVAILABLE

A table of the ^1H chemical shifts of conotoxin pl14a, oligonucleotide primers, the effect of 10 μM pl14a on neuronal nAChR subtypes, NMR spectra of pl14a, and a Ramachandran plot of the 20 lowest-energy structures of pl14a. This material is available free of charge via the Internet at http://pubs.acs.org.

REFERENCES

1. Terlau, H., Shon, K., Grilley, M., Stocker, M., Stühmer, W., and Olivera, B. M. (1996) Strategy for rapid immobilization of prey by a fish-hunting cone snail, *Nature 381*, 148−151.
2. Olivera, B. M., Gray, W. R., Zeikus, R., McIntosh, J. M., Varga, J., Rivier, J., de Santos, V., and Cruz, L. J. (1985) Peptide neurotoxins from fish-hunting cone snails, *Science 230*, 1338−1343.
3. Olivera, B. M. (2002) *Conus* venom peptides: Reflections from the biology of clades and species, *Annu. Rev. Ecol. Syst. 33*, 25−42.
4. Olivera, B. M. (1997) *Conus* venom peptides, receptor and ion channel targets and drug design: 50 million years of neuropharmacology (E. E. Just Lecture, 1996), *Mol. Biol. Cell 8*, 2101−2109.
5. Duda, T. F., Jr., Kohn, A. J., and Palumbi, S. R. (2001) Origins of diverse feeding ecologies within *Conus*, a genus of venomous marine gastropods, *Biol. J. Linn. Soc. 73*, 391−409.
6. Röckel, D., Korn, W., and Kohn, A. J. (1995) *Manual of the Living Conidae, Vol. I: Indo-Pacific Region*, Verlag Christa Hemmen, Wiesbaden, Germany.
7. Massilia, G. R., Schininà, M. E., Ascenzi, P., and Polticelli, F. (2001) Contryphan-Vn: A novel peptide from the venom of the Mediterranean snail *Conus ventricosus*, *Biochem. Biophys. Res. Commun. 288*, 908−913.
8. Sudarslal, S., Singaravadivelan, G., Ramasamy, P., Ananda, K., Sarma, S. P., Sikdar, S. K., Krishnan, K. S., and Balaram, P. (2004) A novel 13 residue acyclic peptide from the marine snail, *Conus monile*, targets potassium channels, *Biochem. Biophys. Res. Commun. 317*, 682−688.
9. Kauferstein, S., Huys, I., Kuch, U., Melaun, C., Tytgat, J., and Mebs, D. (2004) Novel conopeptides of the I-superfamily occur in several clades of cone snails, *Toxicon 44*, 539−548.
10. Ellison, M., McIntosh, J. M., and Olivera, B. M. (2003) α-Conotoxins ImI and ImII: Similar α7 nicotinic receptor antagonists act at different sites, *J. Biol. Chem. 278*, 757−764.
11. Fan, C.-X., Chen, X.-K., Zhang, C., Wang, L.-X., Duan, K. L., He, L. L., Cao, Y., Liu, S.-Y., Zhong, M.-N., Ulens, C., Tytgat, J., Chen, J.-S., Chi, C.-W., and Zhou, Z. (2003) A novel conotoxin from *Conus betulinus*, κ-BtX, unique in cysteine pattern and in function is a specific BK channel modulator, *J. Biol. Chem. 278*, 12624−12633.
12. McIntosh, J. M., Yoshikami, D., Mahe, E., Nielsen, D. B., Rivier, J. E., Gray, W. R., and Olivera, B. M. (1994) A nicotinic acetylcholine receptor ligand of unique specificity, α-conotoxin ImI, *J. Biol. Chem. 269*, 16733−16739.
13. Abogadie, F. C., Ramilo, C. A., Corpuz, G. P., and Cruz, L. J. (1990) Biologically active peptides from *Conus quercinus*, a worm-hunting species, *Trans. Natl. Acad. Sci. Technol., Repub. Philipp. 12*, 219−232.
14. Braga, M. C. V., Katsuhiro, K., Portaro, F. C. V., De Freitas, J. C., Yamane, T., Olivera, B. M., and Pimenta, D. C. (2005) Mass spectrophotometric and high performance liquid chromatography profiling of the venom of the Brazilian vermivorous mollusk *Conus regius*: Feeding behavior and identification of one novel conotoxin, *Toxicon 45*, 113−122.
15. Loughnan, M. L., Nicke, A., Jones, A., Adams, D. J., Alewood, P. F., and Lewis, R. J. (2004) Chemical and functional identification and characterization of novel sulfated α-conotoxins from the cone snail *Conus anemone*, *J. Med. Chem. 47*, 1234−1241.

16. Moller, C., Rahmankhah, S., Lauer-Fields, J., Bubis, J., Fields, G. B., and Mari, F. (2005) A novel conotoxin framework with a helix-loop-helix (Cs α/α) fold, *Biochemistry 44*, 15986−15996.
17. Aguilar, M. B., Lopez-Vera, E., Imperial, J. S., Falcon, A., Olivera, B. M., and Heimer de la Cortera, E. P. (2005) Putative γ-conotoxins in vermivorous cone snails: The case of *Conus delessertii*, *Peptides 26*, 23−27.
18. Terlau, H., and Olivera, B. M. (2004) *Conus* venoms: A rich source of novel ion channel-targeted peptides, *Physiol. Rev. 84*, 41−68.
19. Espiritu, D. J. D., Watkins, M., Dia-Monje, V., Cartier, G. E., Cruz, L. J., and Olivera, B. M. (2001) Venomous cone snails: Molecular phylogeny and the generation of toxin diversity, *Toxicon 39*, 1899−1916.
20. Alewood, P. F., Alewood, D., Miranda, L. P., Love, S., Meutermans, W. D. F., and Wilson, D. (1997) Rapid in situ neutralization protocols for Boc and Fmoc solid-phase chemistries, *Methods Enzymol. 289*, 14−29.
21. Manuscript in preparation.
22. Gray, W. R. (1993) Disulfide structures of highly bridged peptides: A new strategy for analysis, *Protein Sci. 2*, 1732−1748.
23. Daly, N. L., Ekberg, J. A., Thomas, L., Adams, D. J., Lewis, R. J., and Craik, D. J. (2004) Structures of μO-conotoxins from *Conus marmoreus*. Inhibitors of tetrodotoxin (TTX)-sensitive and TTX-resistant sodium channels in mammalian sensory neurons, *J. Biol. Chem. 279*, 25774−25782.
24. Rosengren, K. J., Daly, N. L., Plan, M. R., Waine, C., and Craik, D. J. (2003) Twists, knots, and rings in proteins. Structural definition of the cyclotide framework, *J. Biol. Chem. 278*, 8606−8616.
25. Guntert, P., Mumenthaler, C., and Wutrich, K. (1997) Torsion angle dyanmics for NMR structure calculation with the new program DYANA, *J. Mol. Biol. 273*, 283−298.
26. Brunger, A. T., Adams, P. D., and Rice, L. M. (1997) New applications of simulated annealing in X-ray crystallography and solution, *Structure 5*, 325−336.
27. Hutchinson, E. G., and Thornton, J. M. (1996) PROMOTIF: A program to identify and analyze structural motifs in proteins, *Protein Sci. 5*, 212−220.
28. Laskowski, R. A., Rullmannn, J. A., MacArthur, M. W., Kaptein, R., and Thornton, J. M. (1996) AQUA and PROCHECK-NMR: Programs for checking the quality of protein structures solved by NMR, *J. Biomol. NMR 8*, 477−486.
29. Frohman, M. A. (1990) RACE: Rapid amplification of cDNA ends, in *PCR Protocols* (Innis, M. A., Ed.) pp 28−45, Academic Press, San Diego.
30. Cartier, G. E., Yoshikami, D., Gray, W. R., Luo, S., Olivera, B. M., and McIntosh, J. M. (1996) A new α-conotoxin which targets α3β2 nicotinic acetylcholine receptors, *J. Biol. Chem. 271*, 7522−7528.
31. Jacobsen, R. B., Koch, E. D., Lang-Malecki, B., Stocker, M., Verhey, J., van Wagoner, R. M., Vyazovkina, A., Olivera, B. M., and Terlau, H. (2000) Single amino acid substitutions in κ-conotoxin PVIIA disrupt interaction with the *Shaker* K^+ channel, *J. Biol. Chem. 275*, 24639−24644.
32. Horton, R. M., Manfredi, A. A., and Conti-Tronconi, B. M. (1993) The 'embryonic' γ subunit of the nicotinic acetylcholine receptor is expressed in adult extraocular muscle, *Neurology 43*, 983−986.
33. Cruz, L. J., Johnson, D. S., and Olivera, B. M. (1987) Characterization of the ω-conotoxin target. Evidence for tissue-specific heterogeneity in calcium channel types, *J. Biol. Chem. 26*, 820−824.
34. Wutrich, K. (1986) *NMR of Proteins and Nucleic Acids*, Wiley-Interscience, New York.
35. Eipper, B. A., Perkins, S. N., Hustin, E. J., Johnson, R. C., Keutmann, H. T., and Mains, R. E. (1991) Peptidyl-α-hydroxylglycine α-amidating lyase, *J. Biol. Chem. 266*, 7827−7833.
36. Olivera, B. M., Rivier, J., Clark, C., Ramilo, C. A., Corpuz, G. P., Abogadie, F. C., Mena, E. E., Woodward, S. R., Hillyard, D. R., and Cruz, L. J. (1990) Diversity of *Conus* neuropeptides, *Science 249*, 257−263.
37. Groebe, D. R., Gray, W. R., and Abramson, S. N. (1997) Determinants involved in the affinity of α-conotoxins GI and SI for the muscle subtype of nicotinic acetylcholine receptors, *Biochemistry 36*, 6469−6474.
38. Shon, K., Stocker, M., Terlau, H., Stühmer, W., Jacobsen, R., Walker, C., Grilley, M., Watkins, M., Hillyard, D. R., Gray, W. R., and Olivera, B. M. (1998) κ-Conotoxin PVIIA: A peptide inhibiting the Shaker K^+ channel, *J. Biol. Chem. 273*, 33−38.
39. Ferber, M., Sporning, A., Jeserich, G., DeLa Cruz, R., Watkins, M., Olivera, B. M., and Terlau, H. (2003) A novel *Conus* peptide ligand for K^+ channels, *J. Biol. Chem. 278*, 2177−2183.
40. Bayrhuber, M., Vijayan, V., Ferber, M., Graf, R., Korukottu, J., Imperial, J., Garrett, J. E., Olivera, B. M., Terlau, H., Zweckstetter, M., and Becker, S. (2005) Conkunitzin-S1 is the first member of a new Kunitz-type neurotoxin family: Structural and functional characterization, *J. Biol. Chem. 180*, 21246−21255.
41. Imperial, J. S., Silverton, N., Olivera, B. M., Bandyopadhyay, P. K., Sporning, A., Ferber, M., and Terlau, H. (2006) Using venom chemistry to reveal the origins of fish-hunting in cone snails, *Proc. Am. Philos. Soc.* (in press).
42. Cotton, J., Crest, M., Bouet, F., Alessandri, N., Gola, M., Forest, E., Karlsson, E., Castaneda, O., Harvey, A. L., Vita, C., and Menez, A. (1997) A potassium-channel toxin from the sea anemone *Bundosoma granulifera*, an inhibitor for Kv1 channels. Revision of the amino acid sequence, disulfide-bridge arrangement, chemical synthesis and biological activity, *Eur. J. Biochem. 244*, 192−202.
43. Fajloun, Z., Carlier, E., Lecomte, C., Geib, S., Di Luccio, E., Bichet, D., Mabrouk, K., Rochat, H., De Waard, M., and Sabatier, J. M. (2000) Chemical synthesis and characterization of Pi1, a scorpion toxin from *Pandinus imperator* active on K^+ channels, *Eur. J. Biochem. 267*, 5149−5155.
44. Chagot, B., Pimentel, C., Dai, L., Pil, J., Tytgat, J., Nakajima, T., Corzo, G., Darbon, H., and Ferrat, G. (2005) An unusual fold for potassium channel blockers: NMR structure of three toxins from the scorpion *Opisthacanthus madagascariensis*, *Biochem. J. 388*, 263−271.
45. Srinivasan, K. N., Sivaraja, V., Huys, I., Sasaki, T., Cheng, B., Kumar, T. K. S., Sato, K., Tytgat, J., Yu, C., San, B. C. C., Ranganathan, S., Bowie, H. J., Kini, R. M., and Gopalakrishnakone, P. (2002) κ-Hefutoxin1, a novel toxin from the scorpion *Heterometrus fulvipes* with unique structure and function, *J. Biol. Chem. 277*, 30040−30047.
46. Dauplais, M., Lecoq, A., Song, J., Cotton, J., Jamin, N., Gilquin, B., Roumestand, C., Vita, C., de Medieros, C. L. C., Rowan, E. G., Harvey, A. L., and Menez, A. (1997) On the convergent evolution of animal toxins, *J. Biol. Chem. 272*, 4302−4309.
47. Gilquin, B., Racape, J., Wrisch, A., Visan, V., Lecoq, A., Grissmer, S., Menez, A., and Gasparini, S. (2002) Structure of the BgK−Kv1.1 complex based on distance restraints identified by double mutant cycles, *J. Biol. Chem. 277*, 37406−37413.
48. Verdier, L., Al-Sabi, A., Rivier, J. E. F., and Olivera, B. M. (2005) Identification of a novel pharmacophore for peptide toxins interacting with K^+ channels, *J. Biol. Chem. 280*, 21246−21255.
49. Mouhat, S., Mosbah, A., Visan, V., Wulff, H., Delepierre, M., Darbon, H., Grissmer, S., De Waard, M., and Sabatier, J. (2004) The functional dyad of scorpion toxin Pi1 is not itself a prerequisite for toxin binding to the voltage-gated Kv1.2 potassium channels, *Biochem. J. 377*, 25−36.
50. Johnson, D. S., Martinez, J., Elgoyhen, A. B., Heinemann, S. F., and McIntosh, J. M. (1995) α-Conotoxin ImI exhibits subtype-specific nicotinic acetylcholine receptor blockade: Preferential inhibition of homomeric α7 and α9 receptors, *Mol. Pharmacol. 48*, 194−199.
51. Luo, S., Kulak, J. M., Cartier, G. E., Jacobsen, R. B., Yoshikami, D., Olivera, B. M., and McIntosh, J. M. (1998) α-Conotoxin AuIB selectively blocks α3β4 nicotinic acetylcholine receptors and nicotine-evoked norepinephrine release, *J. Neurosci. 18*, 8571−8579.
52. McIntosh, J. M., Plazas, P. V., Watkins, M., Gomez-Casati, M. E., Olivera, B. M., and Elgoyhen, A. B. (2005) A novel κ-conotoxin, PeIA, cloned from *Conus pergrandis*, discriminates between rat κ9κ10 and κ7 nicotinic cholinergic receptors, *J. Biol. Chem. 280*, 30107−30112.
53. Azam, L., Dowell, C., Watkins, M., Stitzel, J. A., Olivera, B. M., and McIntosh, J. M. (2005) κ-Conotoxin BuIA, a novel peptide from *Conus bullatus*, *J. Biol. Chem. 280*, 80−87.
54. Olamendi-Portugal, T., Somodi, S., Fernandez, J. A., Zamudio, F. Z., Becerril, B., Varga, Z., Panyi, G., Gaspar, R., and Possani, L. D. (2005) Novel α-KTx peptides from the venom of the scorpion *Centruroides elegans* selectively blockade Kv1.3 over IKCa1 K^+ channels of T cells, *Toxicon 46*, 418−429.
55. Miller, C. (1995) The charybdotoxin family of K^+ channel-blocking peptides, *Neuron 15*, 5−10.

56. Selisko, B., Garcia, C., Becerril, B., Gomez-Lagunas, F., Garay, C., and Possani, L. D. (1998) Cobatoxins 1 and 2 from *Centruroides noxius* Hoffmann constitute a subfamily of potassium-channel-blocking scorpion toxins, *Eur. J. Biochem. 254*, 468−479.
57. Dudina, E. E., Korolkova, Y. V., Bocharova, N. E., Koshelev, S. G., Egorov, T. A., Huys, I., Tytgat, J., and Grishin, E. V. (2001) OsK2, a new selective inhibitor of Kv1.2 potassium channels purified from the venom of the scorpion *Orthochirus scrobiculosus*, *Biochem. Biophys. Res. Commun. 286*, 841−847.
58. Peter, M. J., Varga, Z., Hajdu, P., Gaspar, R. J., Damjanovich, S., Horjales, E., Possani, L. D., and Panyi, G. (2001) Effect of toxins Pi2 and Pi3 on human T lymphocyte Kv1.3 channels: The role of glu7 and lys24, *J. Membr. Biol. 179*, 13−25.
59. Abdel-Mottaleb, Y., Coronas, F. V., de Roodt, A. R., Possani, L. D., and Tytgat, J. (2006) A novel toxin from the venom of the scorpion *Tityus trivittatus* is the first member of a new α-KTX subfamily, *FEBS Lett. 580*, 592−596.
60. Huys, I., Xu, C.-Q., Wang, C.-Z., Vacher, H., Martin-Eauclaire, M.-F., Chi, C.-W., and Tytgat, J. (2004) BmTx3, a scorpion toxin with two putative functional faces separately active on A-type K^+ and HERG currents, *Biochem. J. 378*, 745−752.

BI060263R